TRANSPORT PROBLEMS 2016 Volume 11 Issue 3
PROBLEMY TRANSPORTU DOI: 10.20858/tp.2016.11.3.2

cranes; aluminium alloys; steel; load-carrying structure; strength

Damian GĄSKA*, Tomasz HANISZEWSKI
Silesian University of Technology, Faculty of Transport
Krasińskiego 8, 40-019 Katowice, Poland
**Corresponding author:* E-mail: damian.gaska@polsl.pl

MODELLING STUDIES ON THE USE OF ALUMINIUM ALLOYS IN LIGHTWEIGHT LOAD-CARRYING CRANE STRUCTURES

Summary. The article presents the results of numerical analysis whose aim was to compare the basic dynamic and strength parameters of lightweight load-carrying crane structures made of aluminium alloys and steel. The analysis covered the typical construction of workshop cranes with a span of 3 to 5 meters, girders in the form of an I-beam and maximum load capacities amounting to 5 tons. The values of stresses, deflections and natural frequencies were compared and then matched with the masses of the various structures. In the simulation a girder model was used and computed by the finite element method.

BADANIA MODELOWE WYKORZYSTANIA STOPÓW ALUMINIUM W USTROJACH NOŚNYCH LEKKICH SUWNIC

Streszczenie. W artykule przedstawiono wyniki analizy numerycznej, której celem było porównanie podstawowych parametrów dynamicznych i wytrzymałościowych ustrojów nośnych lekkich suwnic wykonanych z aluminium i stali. Analizie poddano typowe konstrukcje suwnic warsztatowych o rozpiętości od 3 do 5 metrów, o dźwigarach w postaci dwuteownika i maksymalnych udźwigach wynoszących 5 ton. Porównywano wartości naprężeń, ugięć i częstotliwości drgań własnych, a następnie zestawiono je z masami poszczególnych ustrojów. W symulacji wykorzystano model dźwigara obliczany z wykorzystaniem metody elementów skończonych.

1. INTRODUCTION

Light cranes produced today are used in industry as mobile cargo handling equipment. From a theoretical point of view, they are among the basic machines that are used in the transport of freight. The construction material mainly used for load-carrying structures is steel, but they are also increasingly built from aluminium alloys [1, 2].

An important advantage of such structures is much less weight compared to steel structures. However, the negative consequence is the change of the strength and dynamic parameters. Mechanical vibrations caused by the intermittent work of enforcement mechanisms cause an induction of dynamic loads in each transshipment cycle, which affects both the construction of the device and its operation [3].

Such cranes are easy to transport and install—in most cases human muscle strength without specialized hardware is enough. Another difference from steel load-carrying structures is the method of manufacture. In the case of aluminium alloy, welded joints are avoided and replaced by screw joints

-this increases mobility at the same time as facilitating quick assembly and disassembly. Unfortunately, the influence of welding significantly reduces the strength parameters in the heat-affected zone [4, 5]. In addition, each load-carrying crane structure shall "inform" of any overloads, and cracks cannot propagate immediately [6 - 8]. The advantage of steel in this respect lies mainly in its higher impact strength relative to aluminium alloys; therefore, aluminium structures are used for low-intensity use (crane classes) [9 - 11].

The structure of the analyzed cranes is made of aluminium alloy with magnesium and silicon. Such alloys have good mechanical properties and enhanced corrosion resistance, particularly in water and maritime atmospheres. They are mainly used for medium stressed parts of ships and cranes, as well as in the aerospace industry.

2. MATERIALS AND METHODS

In order to analyze the impact of using aluminium alloys for the construction of crane structures in terms of strength parameters, numerical models of the discussed structure were built. Both the dynamic and static behaviour of the supporting structure were analyzed using Matlab and Abaqus software [12, 13], with particular emphasis on the stresses occurring in the lower flange of the I-beam girder. The stresses occurring there have a decisive influence on the strength of the structure due to the presence of the cumulative phenomenon of general bending and local bending of the lower flange [14].

In the numerical simulation, an I-beam crane girder with a span equal to 3, 4 or 5 m and a maximum capacity of 3 t was used. In the presented model, the construction of headstocks and other unnecessary elements of the crane were omitted. The model was loaded in the middle of its span. The girder had the same design and dimensions for each case, and only the material parameters were modified.

The load-carrying structure was made from ASTM A284 steel and aluminium 6061-T6. Standardized general purpose quadratic shell elements S8R and general purpose quadratic brick elements with reduced integration points C3D20R from Abaqus Software Documentation were used.

The boundary conditions were applied to the reference points, which are combined with the construction by using an MPC beam type connector. Construction of the girder was divided into three parts—two surface types and one as a solid type (in order to shorten the calculation time). These parts were combined with each other by using a shell-to-solid coupling, which connects the side surface of the solid model with the edge of the shell. The load was applied by adding masses to the wheel axles of the hoist by using kinematic coupling constraints. The load at the bottom flange of the girder was made by using node-to-surface type contact elements. Between the contact of the wheel and the surface of the lower flange of the girder, a friction coefficient was used, differing for aluminium alloy and steel (Table 1). In the simulation, gravity as an acceleration value of 9,81 m/s^2 was also applied.

Table 1

Physical and strength properties of construction materials [15]

Property	ASTM A284 steel, grade C	Aluminium 6061-T6; 6061-T651
Density	7,85 g/cm^3	2,70 g/cm^3
Tensile strength, ultimate	415 MPa	310 MPa
Tensile strength, yield	205 MPa	276 MPa
Modulus of elasticity	205 GPa	68,9 GPa
Poisson’s ratio	0,30	0,33
Friction coefficient	0,15	0,30

In the Matlab-Simulink environment, the dynamic model was formulated (Fig. 1) [3]. The physical parameters describing the considered vibrating model were estimated on the basis of the technical

documentation of the overhead travelling crane. Then the numerical experiments with the classical elastic-damping model (Kelvin–Voigt) for the wire rope were performed.

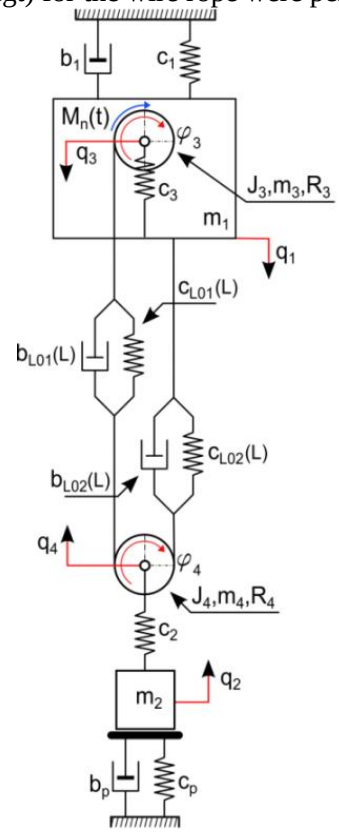

Fig. 1. Simplified phenomenological model of examined overhead travelling crane, which includes Kelvin-Voigt model of wire rope, where: m_1 – reduced mass of girder, m_2 – mass of load, m_3 – mass of the rope drum, m_4 – mass of the pulley, J_3 – mass moment of inertia of the rope drum, J_4 – mass moment of inertia of the pulley, $\dot{q}_1$, $\dot{q}_2$, $\dot{q}_3$, $\dot{q}_4$, $\dot{\varphi}_3$, $\dot{\varphi}_4$ – generalized velocity, c_3 – stiffness coefficient of the cable drum axle, c_2 – stiffness coefficient of hook, c_p – stiffness coefficient of ground, c_1 – stiffness coefficient of girder, c_L – stiffness coefficient of steel wire rope, R_3 – radius of the cable drum, R_4 – radius of the pulley, i_w – gear ratio of pulley blocks, q_1, q_2, q_3, q_4, φ_3, φ_4 – generalized displacements, b_1 – girder damping ratio, b_p – ground damping ratio, b_L – steel wire rope damping ratio, $M_n(t)$ - drive torque of rope drum

Rys. 1. Uproszczony model fenomenologicznyczny mechanizmu podnoszenia, zawierający w gałęzi linowej model Kelvina-Voigta, gdzie: m_1 – masa zredukowana ustroju nośnego wraz z masą wciągnika, m_2 – masa ładunku, m_3 – masa bębna, m_4 – masa wielokrążka, J_3 – masowy moment bezwładności bębna linowego, J_4 – masowy moment bezwładności wielokrążka, $\dot{q}_1$, $\dot{q}_2$, $\dot{q}_3$, $\dot{q}_4$, $\dot{\varphi}_3$, $\dot{\varphi}_4$ – prędkości uogólnione, c_3 – sztywność łożysk osi bębna linowego, c_2 – sztywność haka, c_p – sztywność podłoża, c_1 – sztywność ustroju nośnego (dźwigara), c_L – sztywność liny, R_3 – promień bębna, , R_4 – promień krążka, i_w – przełożenie wielokrążka, q_1, q_2, q_3, q_4, φ_3, φ_4 – uogólnione przemieszczenia, b_1 – tłumienie dźwigara, b_p – tłumienie podłoża, b_L – tłumienie liny, $M_n(t)$ – moment napędowy na bębnie

The extortion signal is used as a constant driving torque, corresponding to fast start of the engine without the control system, i.e., the worst case. In accordance with the applicable standard [9], the hoist drive class HD1 for the lifting mechanisms without creep speed was examined. Simulations were carried out using algorithm ode4 with constant step of integration 0,0001 s. Simulations were performed for the load value of 30000 N. The rope stiffness and damping coefficients were defined by the relation that their value depends on the length of the rope [3] (fig 2). The values of simplified phenomenological model parameters of examined overhead travelling crane are shown in Table 2 [3]. Variable damping coefficient of the wire rope strand is taken from the publications [3, 16]:

(1)

$$b_L = 2\xi\sqrt{c_L \cdot m}$$

where: c_L – stiffness coefficient of steel wire rope, b_L – wire rope damping ratio, ξ – dimensionless coefficient according to [16], m – sum of load mass with current steel wire rope mass (depending of its length).

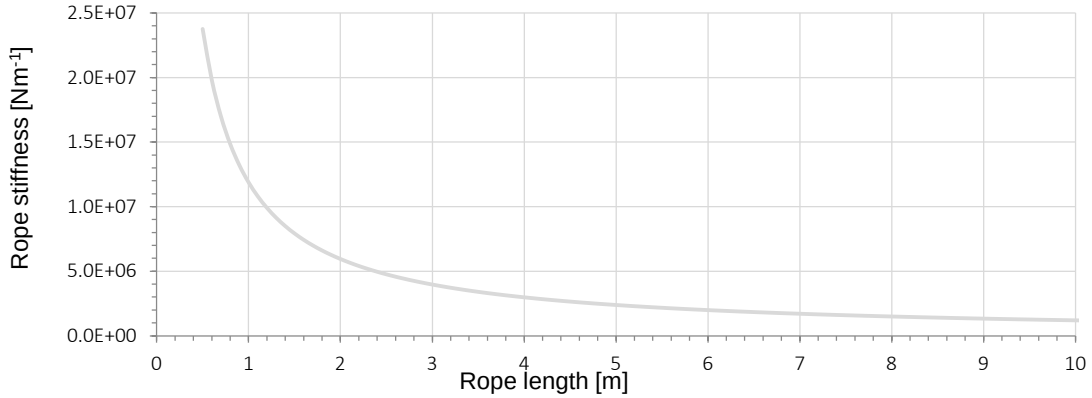

Fig. 2. Ratio between wire rope stiffness and wire rope length, where E_l=0,5E_S [3]
Rys. 2. Zależność sztywności liny od jej długości [3]

Table 2

Physical parameters describing the dynamic system

No.	Symbol	Value	Unit	No.	Symbol	Value	Unit
1	m_1	964	[kg]	9	c_p	2,0e8	[N/m]
2	m_2	5000	[kg]	10	c_3	1,8e8	[N/m]
3	m_3	280	[kg]	11	b_p	1,0e6	[Ns/m]
4	m_4	30	[kg]	12	b_1	2,3e4	[Ns/m]
5	J_3	16,15	[kgm^2]	13	R_3	0,25	[m]
6	J_4	0,294	[kgm^2]	14	R_4	0,14	[m]
7	c_1	4,6e6	[N/m]	15	E_s	2,1e011	[Pa]
8	c_2	2e7	[N/m]	16	E_l	1,155e011	[Pa]

3. RESULTS AND DISCUSSION

Comparison of the results of the numerical analysis for the aluminium alloy and steel is shown in Tables 3 and 4.

Table 3

Results of the numerical analysis for aluminium alloy

Aluminium alloy			
	Girder span		
	3 m	4 m	5 m
Mass, kg	62,07	82,76	103,45
Load capacity, kg	3000	3000	3000
Displacement, mm	2,00	4,56	8,87
Max. stress in wheel-flange contact MPa	194,32	192,99	197,82
Dynamic factor ϕ_2 determined according to [9]	1,295	1,275	1,247
Natural frequency I mode, Hz	12,65	8,38	5,99
Natural frequency II mode, Hz	21,41	20,49	19,19
Natural frequency III mode, Hz	24,08	23,72	22,48

Natural frequency IV mode, Hz	31,06	28,74	25,89

Table 4

Results of the numerical analysis for steel

Steel			
	Girder span		
	3 m	4 m	5 m
Mass, kg	180,45	240,60	300,75
Load capacity, kg	3000	3000	3000
Displacement, mm	0,71	1,62	3,17
Max. stress in wheel-flange contact, MPa	197,2	198,5	198,51
Dynamic factor ϕ_2 determined according to [9]	1,308	1,300	1,286
Natural frequency I mode, Hz	21,62	14,28	10,22
Natural frequency II mode, Hz	27,62	24,81	22,36
Natural frequency III mode, Hz	34,58	29,24	25,36
Natural frequency IV mode, Hz	42,52	41,32	39,59

The natural frequencies are calculated with the use of the FEM model. The values are much lower for the aluminium alloy construction than for the steel one (Table 3, Table 4). This is due to the lower rigidity of the structure. These values are important for the interaction (two-way) with other structural elements of the road, mechanisms or possibly an operator working a crane.

The tables show the maximum value of stress occurring in the contact between the wheel and lower flange of the girder, while Fig. 3 shows the stress values along the lower flange. These values are similar for both the analysed materials and corresponding load capacities. For each of the six stress curves, there are three characteristic points at which, in particular, the stress values are analysed.

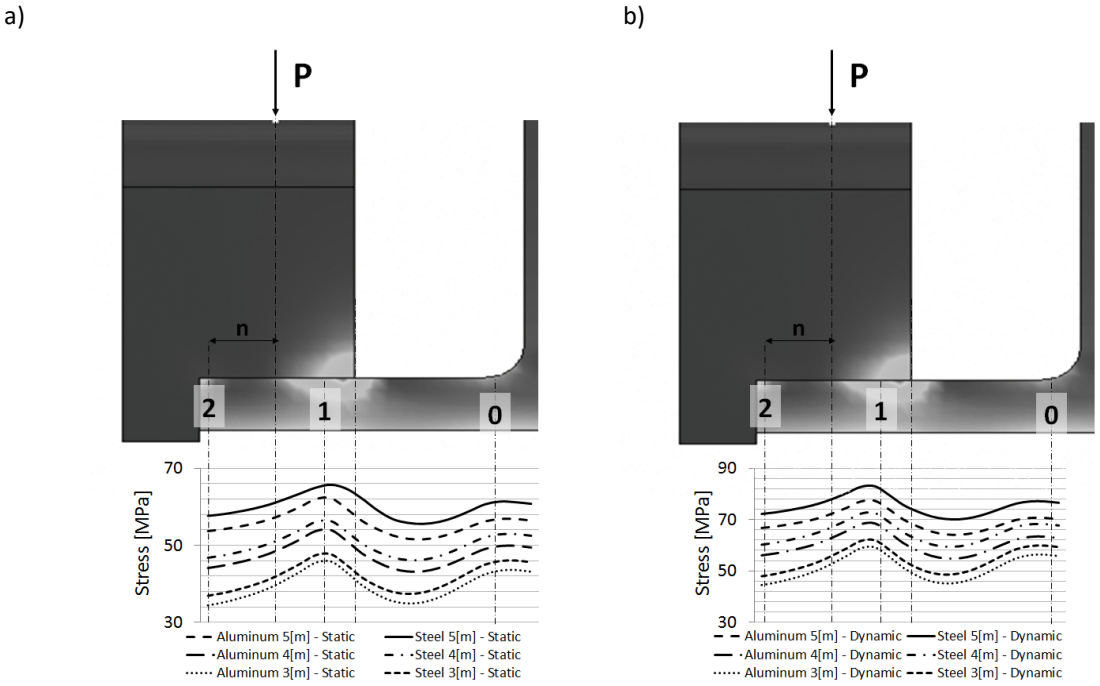

Fig. 3. Dynamic and static values of stress in the bottom flange of the girder (left half) and wheel (bottom half) for steel and aluminium alloy, where: P – force, n – distance between force direction and edge of flange, 0, 1, 2, - characteristic points of the flange

Rys. 3. Porównanie wartości naprężeń w dolnej półce dźwigara (lewa połowa) wraz z kołem wciągnika (dolna część) dla stali i stopów aluminium, gdzie: P – siła, n – odległość pomiędzy kierunkiem przyłożenia siły i krawędzią półki, 0, 1, 2, – punkty charakterystyczne na dźwigarze

As in the case of stress, a situation with dynamic coefficient ϕ_2 is presented [9] (Fig. 4, Table 3, Table 4). This value is mostly related to the characteristics of the hoisting mechanism drive rather than to the behaviour of the load-carrying structure. In the analyzed cases, the same characteristics of the mechanism were simulated for all models.

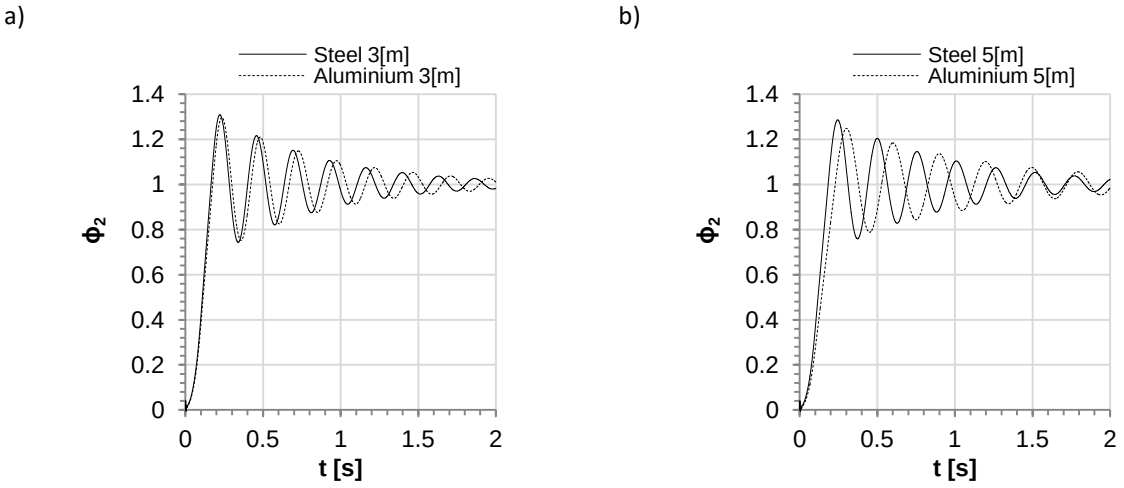

Fig. 4. Dynamic factor changes in the middle of the 3 m and 5 m girder
Rys. 4. Zmiana współczynnika dynamiki podnoszenia dla ustroju z dźwigarem o długościach 3 m i 5 m

A vast difference occurs in the case of the mass of the structures (about three times for each span). This may have important implications for the crane when mounted on a means of transport—sea, air or land. A negative consequence of the three times smaller modulus of elasticity of aluminium alloys compared to steel is the differences between the displacement of the girder centre point (Fig. 5, Table 3, Table 4), the values of the natural frequency, and the acceleration in the middle of the girder span (Fig. 6).

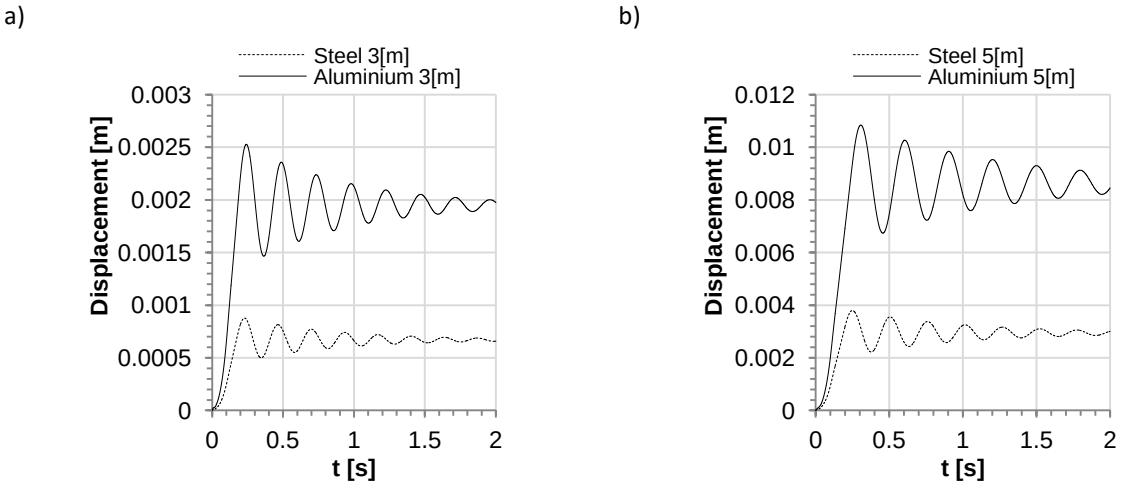

Fig. 5. Displacement in the middle of the 3 m and 5 m girder
Rys. 5. Zmiana przemieszczenia środka dźwigara dla ustroju z dźwigarem o długościach 3 m i 5 m

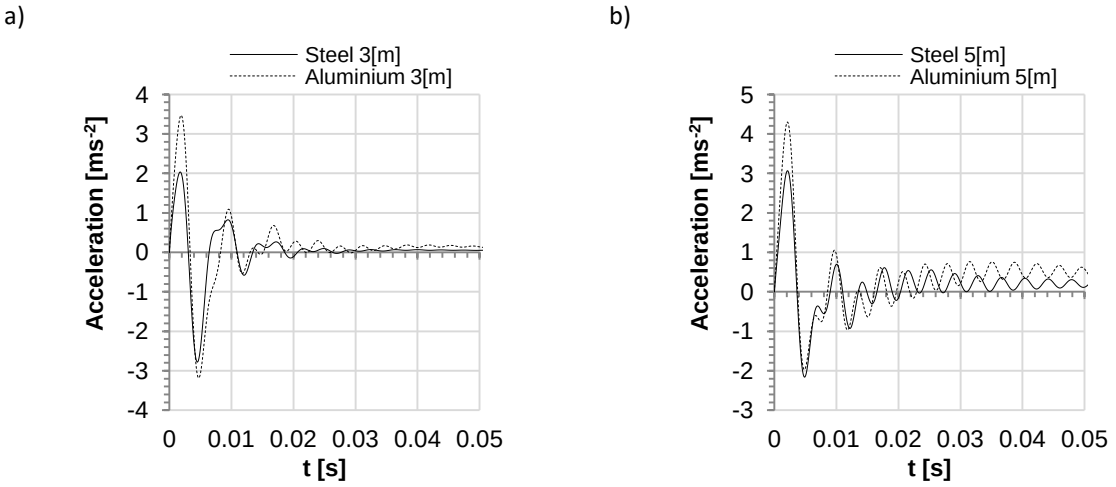

Fig. 6. Acceleration in the middle of the 3 m and 5 m girder
Rys. 6. Zmiana przyspieszenia środka dźwigara dla ustroju z dźwigarem o długościach 3 m i 5 m

The differences in the case of displacement in the middle of the girder span for the steel and aluminium alloy structures are three times to the benefit of the steel. In the case of load-carrying crane structures, this is very important due to the hoisting operations in each working cycle. In addition, the permissible deflections are standardized and, if they are exceeded, the structure has to be reinforced.

4. CONCLUSIONS

Selected aluminium alloys are very good construction materials and suitable for use in lightweight load-carrying crane structures. The main advantage of such structures is the reduced mass with retained strength parameters. Taking into account the dynamic parameters of the analyzed structures, it must be noted that those made of aluminium alloy show much less stiffness. Therefore, for larger bridge spans and larger load capacities, their use may be illegitimate because of the permitted deflection of the girder. Moreover, the structure of aluminium alloy is significantly less resistant to loss of local stability. In the case of A284 steel (Table 1), the difference between ultimate strength and yield tensile strength is 210 MPa. For analyzed aluminum alloy, it is only 34 MPa. Taking into account the fact that the load-carrying structure should "inform" about the overloads, in this case there will not be a lot of warning before the disaster. Another limitation may be economic considerations, which are not included in this publication.

References

1. Urrea, C. & Henríquez, G. & Jamett, M. Development of an expert system to select materials for the main structure of a transfer crane designed for disabled people. *Expert Systems with Applications*. 2015 Vol. 42. P. 691–697.
2. Cieśla, M. Aluminium supplier selection for the automotive parts manufacturer. *Metalurgija*. 2016. Vol. 66. No. 2. P. 237-240.
3. Margielewicz, J. & Haniszewski, T. & Gąska, D. & Pypno, C. *Model studies of cranes hoisting mechanisms*. Katowice: Polish Academy of Science. 2013. 204 p.
4. Piątkowski, J. & Wieszała, R. Microstructure of AlSi17Cu5 alloy after overheating over liquidus temperature. *Metalurgija*. 2015. Vol. 54. No. 1. P. 131-134.
5. Hadryś, D. & Węgrzyn, T. & Piwnik, J. Plastic properties of fine-grained WMD after micro-jet cooling. *Arch. Metall. Mater*. 2014. Vol. 59. No. 3. P. 919-923.

6. Burdzik, R. & Stanik, Z. & Warczek, J. Method of assessing the impact of material properties on the propagation of vibrations excited with a single force impulse. *Arch. Metall. Mater*. 2012. Vol. 53. No. 2. P. 409-416.
7. Kohut, P. & Gąska, A. & Holak, A. & Ostrowska, K. & Sładek, J. & Uhl, T. & Dworakowski, Z. A structure's deflection measurement and monitoring system supported by a vision system. *Technisches Messen*. 2014. Vol. 81. No. 12. P. 635–643.
8. Haniszewski, T. & Gąska, D. & Margielewicz, J. Mechanical properties identification of steel wire rope with fiber core. *Scientific Journal of Silesian University of Technology. Series Transport*. 2014. Vol. 85. P. 27-35.
9. EN 13001-2:2011: *Crane safety - General design - Part 2: Load actions*.
10. EN 1999 – *Eurocode 9: Design of aluminium structures - Part 1.5: Shell structures*.
11. EN 1090-3 – *Execution of steel structures and aluminium structures - Part 3: Technical requirements for aluminium structures*.
12. Gąska, D. & Pypno, C. Strength and elastic stability of cranes in aspect of new and old design standards. *Mechanika*. 2011. Vol. 17. No. 3. P. 226-231.
13. Bogdevičius, M. & Vika, A. Investigation of the dynamics of an overhead crane lifting process in a vertical plane. *Transport*. 2005. Vol. 20. No. 5. P. 176-180.
14. White, D. & Zureick, A. & Phoawanich, N. & Se-Kwon Jung. *Development of unified equations for design of curved and straight steel bridge I-girders*. School of Civil and Environmental Engineering Georgia Institute of Technology. 2001. 551 p.
15. MatWeb. Available at: http://www.matweb.com.
16. Kim, C.S. & Hong, K.S. & Kim, M.K. Nonlinear robust control of a hydraulic elevator: Experiment-based modeling and two-stage Lyapunov redesign. *Control Engineering Practice*. 2005. Vol. 13 (6). P. 789-803.

Received 11.03.2015; accepted in revised form 24.08.2016